Emerging techniques for elucidating mechanism of action of Deep Brain Stimulation

Kendall H. Lee[1], Su-Youne Chang[1], Dong-Pyo Jang[1], Inyong Kim[1], Stephan Goerss[1], Jamie Van Gompel[1], Paul Min[1], Kanika Arora[1], Michael Marsh[1], Sun Chul Hwang[1], Christopher J. Kimble[2], Paul Garris[3], Charles Blaha[4], and Kevin E. Bennet[2]

[1]Dept. of Neurosurgery, [2]Division of Engineering,Mayo Clinic Rochester; [3]Illinois State University; [4]Dept of Psychology, University of Memphis

Abstract— **Deep brain stimulation (DBS) within the basal ganglia complex is an effective neurosurgical approach for treating symptoms of Parkinson's disease (PD), Essential Tremor, Dystonia, Depression, Obssessive Compulsive Disorder, and Tourette's Syndrome, among others. Elucidating DBS mechanism has become a critical clinical and research goal in stereotactic and functional neurosurgery and in neural engineering. Along with electro-physiological and microdialysis techniques, two additional powerful technologies, notably functional Magnetic Resonance Imaging (fMRI) and *in vivo* neurochemical monitoring have recently been used to investigate DBS-mediated activation of basal ganglia network circuitry. For this purpose, we have previously developed WINCS (Wireless Instantaneous Neurotransmitter Concentration Sensor System), which is an MRI-compatible wireless monitoring device to obtain chemically resolved neurotransmitter measurements at implanted microsensors in a large mammalian model (pig) as well as in human patients. This device supports an array of electrochemical measurements that includes fast-scan cyclic voltammetry (FSCV) for real-time simultaneous *in vivo* monitoring of dopamine and adenosine release at carbon-fiber microelectrodes as well as fixed potential amperometry for monitoring of glutamate at enzyme-linked biosensors. In addition, we have utilized fMRI to investigate subthalamic nucleus (STN) DBS activation in the pig with 3Tesla MR scanner. We demonstrate the activation of specific basal ganglia circuitry during STN DBS using both fMRI and FSCV in the pig model. Our results suggest that fMRI and electrochemistry are important emerging techniques for use in elucidating mechanism of action of DBS.**

I. INTRODUCTION

There has been a significant increase in the application of restorative neurosurgical techniques such as electrical stimulation of specific brain nuclei, known commonly as deep brain stimulation (DBS). Indeed, there has been more than 85,000 patients with DBS implantations and DBS is now FDA approved for several neurological disorders, such as Parkinson's Disease (PD), Essential Tremor (ET), dystonia, and obsessive-compulsive disorder (Benabid et al., 1996; Greene, 2005, Greenberg et al., 2006).

While DBS of the GPi is also effective in the treatment of PD, the subthalamic nucleus (STN) is the most common target for PD,

ameliorating the cardinal PD symptoms of akinesia, rigidity, and tremor (Limousin et al., 1998). Despite well established clinical efficacy, the mechanism of DBS is incompletely understood. Because ablative surgery is similarly effective for treating PD and ET, the stimulation-evoked silencing of pathologically hyperactive neurons was initially postulated as the primary mechanism. This notion was further supported by early work measuring electrophysiology during DBS (Benazzouz, 1995; Beurrier et al., 2001). However, more recent studies have reported activation of output nuclei (Shon et al., 2010b). This paradox has apparently been resolved by mathematical models suggesting that, because of dissimilar excitability of neural elements, soma inhibition and axonal activation are both expected at the DBS electrode site (McIntyre et al., 2004).

The axonal activation hypothesis (Grill et al., 2004; McIntyre et al., 2004) has enormous implications for the DBS mechanism of action. Indeed, DBS should evoke changes in neural activity and neurotransmission in interconnected structures within the basal ganglia complex that ultimately underlie clinical benefit. Nevertheless, our understanding of these distal effects of DBS remains far from complete, in large part because of the technical difficulties in combining measurement modalities for global assessment of neural activity and chemical-specific sensing. Here we describe the use of fMRI and electrochemical monitoring using wireless instantaneous neurotransmitter concentration sensor system (WINCS) to help elucidate the mechanism of action of DBS.
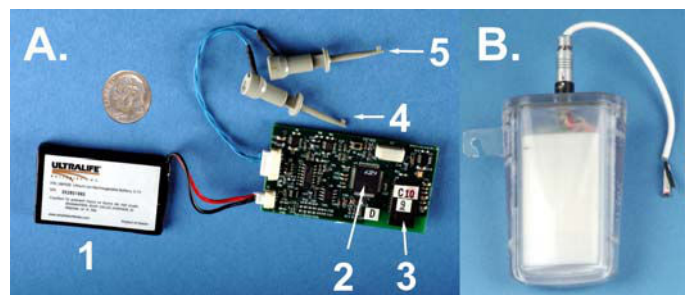

Fig. 1. (**A.**) battery (1), microprocessor (2), Bluetooth transmission chip, (3) electrochemical recording electrode lead (4), and reference electrode lead (5) of the WINCS device. (**B.**) WINCS device encased in its sterilizable polycarbonate case.

II. METHODS

WINCS: For neurochemical monitoring, we have developed a device called the Wireless Instantaneous Neurotransmitter Concentration System (WINCS) designed in compliance with FDA standards for medical electrical device safety (Fig. 1). The WINCS device is capable of monitoring the release of a variety neurochemicals during DBS, using the electroanalytical techniques fast-scan cyclic voltammetry (FSCV) at carbon fiber microelectrode (CFM) and fixed potential amperometry (FPA) at enzyme-linked biosensors. We have tested these two techniques extensively in an inexpensive large animal model (pig) as a prelude to studies in human patients. Presently, we have established our ability to measure *in vivo* dopamine and adenosine (Fig. 2) with CFMs and adenosine and glutamate with an enzyme-linked biosensor during DBS (Agnesi et al., 2009; Bledsoe et al., 2009; Shon et al., 2010a; 2010b).
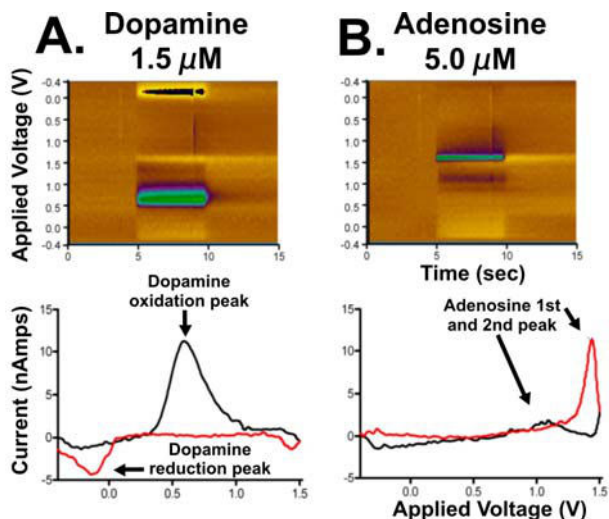
Fig. 2. Detection of dopamine and adenosine using WINCS-based FSCV at a CFM *in vitro*. The color plots show the detection of 1.5 μM dopamine (**A.**), 5.0 μM adenosine (**B.**). The applied potential waveform was scanned from -0.4 to +1.5 V and back to -0.4 V at 400 V/s every 100 msec. Below are shown representative voltammograms. The black lines indicate the current recorded by the forward-going potential from -0.4 V to +1.5 V, and the red lines by the reverse-going potential from +1.5 to -0.4 V. Dopamine and adenosine (1st peak) exhibit unique voltammetric oxidation peaks (+0.6 and +1.5 V, respectively) and thus, can be easily co-detected at the same time.

Animal Studies: The animal experiments were performed in accordance with NIH guidelines and approved by the Mayo Clinic Institutional Animal Care and Use Committee. Male pigs, weighing 26 - 30 kg, were initially sedated with Telazol (5 mg/kg i.m.) and xylazine (2 mg/kg i.m.), then intubated with endo-tracheal tube and ventilated with a artificial ventilator, then maintained with isoflurane (1%) for the remaining experimental procedure. In the prone position, the pig was placed in a MRI-compatible stereotactic head frame. A localizer box was then attached onto the head frame to create nine fiducials to enable localization of MR images in stereotactic space. For fMRI and preoperative targeting of the STN, MRI was performed with a General Electric Signa 3.0 T system. The DICOM image data were then transferred to a stereotactic planning computer and the anterior commissure - posterior commissure line identified on the MR images. Using COMPASS navigational software, MRI data was then merged with a pig atlas and stereotactic coordinates for the DBS electrode implantation trajectory defined.

Thereafter, in the operating room a large midline incision of the skin was made to expose the cranial landmarks of bregma and lambda. This was followed by a burr hole made on the skull in line with our trajectory coordinates. A tungsten extracellular microelectrode (0.5-1.0 MΩ), mounted onto a microdrive, was then lowered using the same trajectory for the DBS electrode obtained by the navigation software to identify the final dorsoventral coordinates of the STN. Following electrophysiologic confirmation of the STN coordinates, a Medtronic 3389 human DBS electrode was then implanted into the STN target. The pig was then returned to the MRI scanner for postoperative confirmation of the placement of the DBS electrode and fMRI studies.

FSCV recordings during STN DBS evoked striatal dopamine release were performed using the wireless instantaneous neurotransmitter concentration system (WINCS) with CFM in the striatum. FSCV not only supports sub-sec measurements at a CFM, but additionally provides a chemical signature in the form of a background-subtracted voltammogram to identify the chemical origin of the signal. FSCV parameters for dopamine measurements consisted of a -0.4 V rest potential, 1.5 V peak potential, 400 V/s scan rate, and 10 Hz scan application. In addition, to complete the circuit necessary for the FSCV a 14 mm burr hole was drilled on the contralateral side of the skull to allow the placement of an Ag/AgCl reference electrode. In a similar fashion to the DBS electrode, preoperative MRI data combined with the pig atlas were used to define the trajectory and final stereotactic coordinates for implantation of the CFM electrode into the center of the head of the caudate.

We have incorporated two features into our pig preparation that are essential for fMRI and neurochemical recordings: a custom-designed MRI-compatible pig frame (Fig. 3A) and modified MRI-assisted stereotactic coordinate calculation software (Compass) (Fig. 3B). The frame, that can provide MR image-guided stereotactic surgery, was constructed in-house of Delrin and carbon fiber to ensure MRI compatibility. We confirmed the accuracy of our frame and targeting procedure using a test phantom with both Computer Tomography (CT) and MRI. Electrode manipulators same as those used for human DBS surgery are attachable to the Leksell stereotactic arc which is then attached to the pig frame. The Compass navigational software that we use for image-guided human stereotactic surgery to co-register a human atlas to the patient MR image has also been modified to co-register the pig stereotactic atlas (Felix et al., 1989) to MR images of individual pig brains (Fig. 3C). We routinely utilized extracellular electrophysiological recording procedures similar to those used in human DBS surgery to determine the final dorsoventral coordinates of the STN, our preoperative MR image-guided procedures provide trajectory coordinates (AP and ML) for implantation of a DBS electrode within regions of the STN of the pig (Fig. 3D).
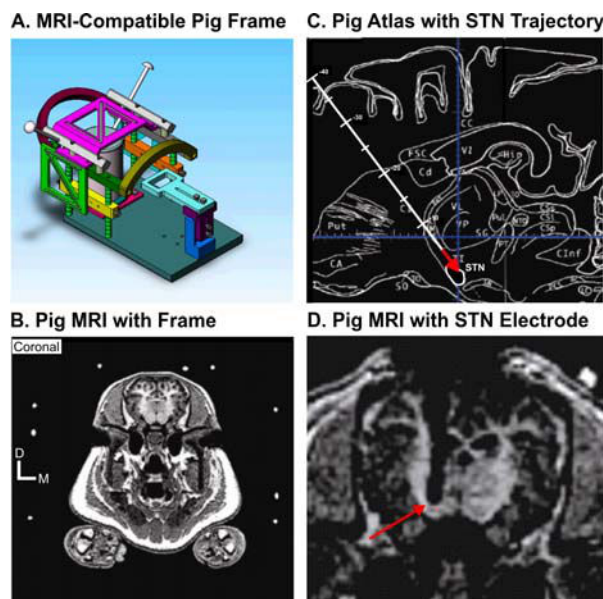

Fig. 3. Pre-operative calculation of the trajectory coordinates for accurate implantation of DBS electrodes in the STN of the pig. **A.** MRI-compatible stereotactic head frame for the pig. **B.** Coronal MRI of pig brain and corresponding fiducials (white circles) on head frame. **C.** Stereotaxic atlas overlaid onto DBS electrode trajectory calculated using MRI-coupled Compass navigational software. **D.** Coronal MRI of pig brain and indwelling relatively large Medtronic 3389 human DBS electrode

III. Results

Parametric and pharmacological analysis of STN DBS on dopamine release. DBS in clinical applications typically involves varying three stimulus pulse parameters: (**1**) intensity, (**2**) frequency, and (**3**) width. These DBS parameters are applied with presently FDA-approved devices in the form of charge-balanced constant-voltage pulses. In our studies in the pig, we tested several variations in DBS parameters with a Medtronic 3389 electrode (contact 0 active) implanted in the STN (n=5 pigs). The majority of these variations in stimulation parameters were within what are regarded as clinically effective in the treatment of PD with STN electrode implants. As shown in Fig. 4A, while holding the stimulation frequency and pulse duration constant (120 Hz, 0.5 msec), increasing pulse intensity from 1 to 7 V resulted in a sigmoidal-like increase in CN dopamine release recorded at CFMs using FSCV. In contrast, with stimulation and pulse width held constant (3 V, 0.5 msec), the magnitude of evoked dopamine release attained a plateau within the test frequencies of 120 to 240 Hz (Fig. 4B). With stimulation frequency and intensity held constant at 120 Hz and 3 V, respectively, increasing the stimulus pulse width from 0.1 to 0.6 msec also resulted in a sigmoidal-like increase in dopamine release (Fig. 4C).

An important feature of these results is that we are able to detect significant increases in dopamine release utilizing "therapeutic" stimulation parameters (3.0 V charge balanced, 0.1 msec pulses at 130 Hz). An additional observation is that the magnitude of STN-evoked dopamine release using a pulse duration of 0.1 msec was significantly smaller compared to responses observed with higher pulse durations that are not routinely used in human STN DBS (e.g., 0.3 and 0.6 msec). Although our pig data show that longer pulse durations elicit maximal evoked-dopamine release, it is highly unlikely that these relatively high evoked increases in extracellular CN dopamine concentrations are physiologically meaningful. If anything, they may be expected to produce cognitive deficits and other deleterious side effects in humans.
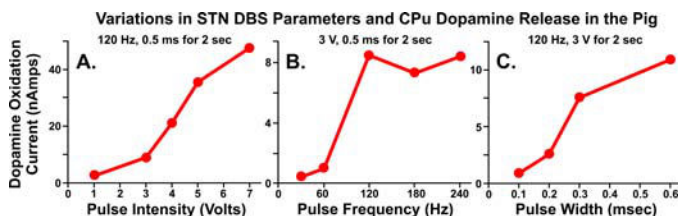
Fig. 4. Dependency of the magnitude of dopamine release recorded at CFMs in the CN of the pig during STN stimulation with varying (**A.**) pulse intensities (1-7 V), (**B.**) pulse frequencies (30-240 Hz), and (**C.**) pulse widths (0.1-0.6 msec). Stimulation parameters held constant during each test are shown above each corresponding graph.

fMRI in the Pig. After completing safety tests, we implanted a Medtronic 3389 DBS electrode into the electrophysiologically identified dorsal STN of the pig (n=5 animals) and secured it in place with a bone secure system. After implantation of this electrode, the subject was transferred to the 3T MR suite. fMRI examinations were performed using a simple block-style paradigm that alternated between the stimulator-off condition and the stimulator-on condition using DBS parameters (3V, 0.5 msec pulse

width at 120 Hz) similar to that used in our parametric studies above (see Fig. 4) that effectively evoked dopamine release in the pig CN. There were five 30-sec stimulator-off epochs and four 30-sec stimulator-on epochs. In this fMRI study, the ipsilateral head/body of the CN was clearly activated by STN DBS of contacts 0-negative and 1-positive as shown in Fig. 5 (yellow arrow). It is important to note, that there was no activation seen in the tail of caudate (tCN, white arrow, Fig. 5D).
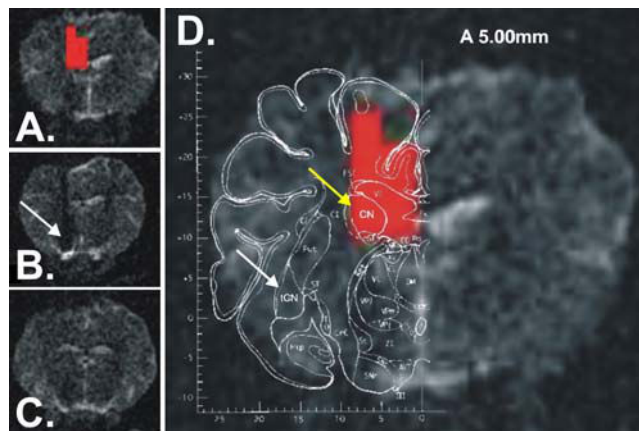
Fig. 5. fMRI test in the pig. Activation of the Medtronic 3389 human DBS electrode implanted into left side of the STN elicited clear activation in the ipsi-lateral region of the CN (**A.**). fMR image of the area of DBS electrode implant (**B.**, white arrow). fMR image og the region posterior to the DBS electrode showing no BOLD contrast increase (**C.**). fMR image blowup of (A.) overlaid on the pig atlas (yellow arrow corresponds to the head/body of the CN activated by STN DBS, whereas the white arrow corresponds to the tail of the CN, tCN not activated by STN DBS) (Felix et al., 1989) (**D.**).

IV. Discussion

We contend that characterization of the understudied region-specific effects of DBS on neurotransmission will provide a deeper understanding of its corrective actions on dysfunctional brain processing, and consequently its therapeutic effects in the patient. This basic knowledge will ultimately be critical to the further development of DBS technology and surgical procedures to produce significant improvement in patient outcome. It is clear that the emerging techniques of fMRI and FSCV will be important in achieving these goals. The axonal activation hypothesis has caused a paradigm shift in how we approach DBS mechanisms of action. As opposed to a predominant effect of local inhibition at the stimulation site, the prevailing effect appears to be excitation of efferent target neurons and subsequent changes in neural network activity and neurotransmitter release in the basal ganglia complex. Despite what appears to be growing acceptance of this general scheme, however, which regions are affected, how they are affected, and what neurotransmitters mediate these changes, remain largely unanswered. This major hurdle for establishing the functional anatomical and identification of the critical neurotransmitters involved in STN DBS is technical, as imaging of brain structures and chemical-specific neurotransmitter release is required.

Given the strong electrophysiological and imaging evidence for the axonal activation hypothesis, it is not surprising that preclinical studies have shown neurotransmitter release in various STN efferent targets during STN DBS. Using the technique of

microdialysis, which physically removes analyte from brain extracellular fluid for *ex vivo* analysis, Windels and colleagues (2000; 2003) have shown in rats that STN DBS significantly increased glutamate and GABA release in the GPe and SNr, respectively. However, the relatively large size of microdialysis probes have been shown to disrupt tissue in the immediate vicinity of the probe resulting in underestimations of extracellular dopamine levels compared to alternative measurement techniques that utilize chemical microsensors (Clapp-Lilly et al., 1999). We thus contend that approaches alternative to microdialysis will be necessary to assess striatal dopamine release during STN DBS. Indeed, chemical microsensors, which offer a smaller probe (5 to 10 μm versus 200 to 400 μm diameter for microdialysis probes), have already shown dopamine release in the striatum evoked by STN DBS in the intact and parkinsonian rat 6-OHDA model (Lee et al., 2006; Blaha et al. 2006). These latter findings are important on several levels. For example, striatal dopamine release during STN DBS has been difficult to establish with microdialysis (Paul et al., 2000), a result that underscores the need for small probe size in chemical recordings. Additionally, the increase in striatal dopamine release coincides with striatal neural activation during STN DBS as determined by fMRI. Indeed, as shown here, we provide preliminary evidence that STN DBS induces activation in the striatum as assessed by fMRI and striatal dopamine release measured by chemical microsensors under identical conditions

V. REFERENCES

Agnesi F, Tye SJ, Bledsoe JM, Griessenauer CJ, Kimble CJ, Sieck GC, Bennet KE, Garris PA, Blaha CD, and Lee KH (2009) Wireless instantaneous neurotransmitter concentration system (WINCS)-based amperometric detection of dopamine, adensoine, and glutamate for intraoperative neurosurgical monitoring. **J Neurosurg**, 2009 in Press.

Benabid AL, Pollak P, Gao D, Hoffmann D, Limousin P, Gay E, Payen I, and Benazzouz A (1996) Chronic electrical stimulation of the ventralis intermedius nucleus of the thalamus as a treatment of movement disorders. J Neurosurg 84(2): 203-214

Benazzouz A, Piallat B, Pollak P, Benabid AL (1995) Responses of substantia nigra pars reticulata and globus pallidus complex to high frequency stimulation of the subthalamic nucleus in rats: electrophysiological data. Neurosci Lett 189:77-80.

Beurrier C, Bioulac B, Audin J, Hammond C (2001) High-frequency stimulation produces a transient blockade of voltage-gated currents in subthalamic neurons. J Neurophysiol 85:1351-1356.

Bezzi P, Carmignoto G, Pasti L, Vesce S, Rossi D, Rizzini BL, Pozzan T, and Volterra A (1998) Prostaglandins stimulate calcium-dependent glutamate release in astrocytes. Nature 391: 281-285

Bezzi P, Vesce S, Panzarasa P, and Volterra A (1999) Astrocytes as active participants of glutamatergic function and regulators of its homeostasis. Adv Exp Med Biol 468:69-80

Blaha CD, Lester DB, Ramsson ES, Lee KH and Garris PA (2008) Striatal dopamine release evoked by subthalamic stimulation in intact and 6-OHDA-lesioned rats: Relevance to deep brain stimulation in Parkinson's Disease. In: Monitoring Molecules in Neuroscience. pp. 395-397.

Bledsoe JM, Kimble CJ, Covey DP, Blaha CD, Agnesi F, Mohseni P, Whitlock S, Johnson DM, Horne A, Bennet KE, Lee KH, and Garris PA (2009) Development of wireless instantaneous neurotransmitter concentration system (WINCS) for intraoperative neurochemical monitoring using fast-scan cyclic voltammetry. **J Neurosurg**, 2009 in Press.

Cechova S and Venton BJ (2008) Transient adenosine efflux in the rat caudate-putamen. J Neurochem 105: 1253-1263

Clapp-Lilly KL, Roberts RC, Duffy LK, Irons KP, Hu Y and Drew KL (1999) An ultrastructural analysis of tissue surrounding a microdialysis probe. J Neurosci Meth 90:129-42.

Felix B, Leger ME, Albe-Fessard D, Marcilloux JC, Rampin O, Laplace JP (1999) Stereotaxic atlas of the pig brain. Brain Research Bulletin 49:1-137.

Fellin T, Pascual O, and Haydon PG (2006) Astrocytes coordinate synaptic networks: balanced excitation and inhibition Physiology (Bethesda) 21:208-215

Fellin T, Pascual O, Gobbo S, Pozzan T, Haydon PG, and Carmignoto G (2004) Neuronal synchrony mediated by astrocytic glutamate through activation extrasynaptic NMDA receptors. Neuron 43(5): 729-743

Grabb MC, Sciotti VM, Gidday JM, Cohen SA and van Wylen DG (1998) Neurochemical and morphological responses to acutely and chronically implanted brain microdialysis probes. J Neurosci Methods 82: 25-34.

Greenberg BD, Malone DA, Friehs GM, Rezai AR, Kubu CS, Malloy PF, Salloway SP, Okun MS, Goodman WK, Rasmussen SA (2006) Three-year outcomes in deep brain stimulation for highly resistant obsessive-compulsive disorder.[erratum appears in Neuropsychopharmacology. 2006 Nov;31(11):2394]. Neuropsychopharmacology 31:2384-2393.

Greene P (2005) Deep-brain stimulation for generalized dystonia.[comment]. New England Journal of Medicine 352:498-500.

Grill WM, Snyder AN, Miocinovic S (2004) Deep brain stimulation creates an informational lesion of the stimulated nucleus. Neuroreport 15:1137-1140.

Lee KH, Chang S, Roberts DW, and Kim U (2004) Neurotransmitter release from high-frequency stimulation of the sub thalamic nucleus. J. Neurosurg 101(3): 511-517

Lee KH, Hitti FL, Shglinsky MH, Kim U, Leiter JC, and Roberts DW (2005) Abolition of spindle oscillations and 3-Hz absence seizure-like activity in the thalamus by using high-frequency stimulation: potential mechanism of action. J Neurosurg 103(3): 538-545

Lee KH, Blaha CD, Cooper S, Hitti FL, Leiter JC, Roberts DW and Kim U (2006) Dopamine efflux in the rat striatum evoked by electrical stimulation of the subthalamic nucleus: potential mechanism of action in Parkinson's disease, Eur J Neurosci 23:1005-1014.

Limousin P, Krack P, Pollak P, Benazzouz A, Ardouin C, Hoffmann D, Benabid AL (1998) Electrical stimulation of the subthalamic nucleus in advanced Parkinson's disease. New England Journal of Medicine 339:1105-1111.

McIntyre CC, Grill WM, Sherman DL, Thakor NV (2004) Cellular effects of deep brain stimulation: model-based analysis of activation and inhibition. J Neurophysiol 91:1457-1469.

Paul G, Reum T, Meissner W, Marburger A, Sohr R, Morgenstern R, Kupsch A (2000) High frequency stimulation of the subthalamic nucleus influences striatal dopaminergic metabolism in the naive rat. Neuroreport 11:441-444.

Shon YM, Chang SY, Tye SJ, Kimble CJ, Bennet KE, Blaha CD, Lee KH (2010a) Comonitoring of adenosine and dopamine using the Wireless Instantaneous Neurotransmitter Concentration System: proof of principle. J Neurosurg 112:539-548.

Shon YM, Lee KH, Goerss SJ, Kim IY, Kimble C, Van Gompel JJ, Bennet K, Blaha CD, Chang SY (2010b) High frequency stimulation of the subthalamic nucleus evokes striatal dopamine release in a large animal model of human DBS neurosurgery. Neurosci Lett 475:136-140.

Windels F, Bruet N, Poupard A, Feuerstein C, Bertrand A, Savasta M (2003) Influence of the frequency parameter on extracellular glutamate and gamma-aminobutyric acid in substantia nigra and globus pallidus during electrical stimulation of subthalamic nucleus in rats. J Neurosci Res 72:259 -267.

Windels F, Bruet N, Poupard A, Urbain N, Chouvet G, Feuerstein C, Savasta M (2000) Effects of high frequency stimulation of subthalamic nucleus on extracellular glutamate and GABA in substantia nigra and globus pallidus in the normal rat. Eur J Neurosci 12:4141- 4146.